20

Reprinted from Applied Optics, Vol. 24, page 551, February 15, 1985

Establishing fiducials on glancing incidence mirrors

Charles M. Fleetwood, Roger J. Thomas, and Geraldine A. Wright

A method is described for aligning cylindrical glancing incidence mirrors and establishing fiducials prior to axial profile measurements. The residual uncertainty in the absolute axial position is 2.54 μm, and the uncertainty in the absolute radius is 0.812 μm.

I. Introduction

During the polishing and testing of optical components it is necessary to establish a coordinate system so that error measurements can be assigned locations on the element and subsequent measurements compared. Techniques for locating fiducials on normal incidence mirrors during testing are well established.[1–3] Normal incidence mirrors are tested by reflecting light which originates from a source at one conjugate focus to the other conjugate focus and interfering the reflected wave front with a spherical wave front of the same radius of curvature. The fringes thus produced contain information about the deviations of the surface from the theoretical curve as a function of position in a plane perpendicular to the optical axis. A camera which has been focused on the element being tested superposes the fringes onto a photograph of the element, and the deviations can be mapped from the interferogram onto the actual surface. The center and edges of the interferogram correspond to the center and edges of the element. Orientation on the interferograms of elements is found by placing a mark on the optical blank in such a position that it will be recorded on the interferogram and not be removed during subsequent polishing. This allows precise mapping of errors with both radial and azimuthal components from the interferogram onto the element.

Since glancing incidence mirrors are generally off-axis segments or cylinders, the techniques used for normal incidence mirrors are not applicable. Interferograms obtained in the same manner as for normal incidence mirrors record the surface error information in a plane which makes a large angle with the optical surface. This compresses the data axially, as shown in Fig. 1, making it difficult to interpret. Even if the interferogram can be interpreted, the large cosine factors involved in mapping the errors back onto the mirror make the axial positions of the surface deviations very sensitive to small errors in measuring fringe positions on the interferogram. For this reason, mechanical methods are used to measure the axial profile, as described by Fleetwood and Mangus.[4] A method for establishing fiducials on the elements of a Wolter type II telescope during profile measurement, as applied to the 13.7-cm long 20.4-cm diam parabolic element of the Solar Extreme Ultraviolet Telescope and Spectrograph,[5,6] is described. The method may be easily adopted for use on other curves figured on either the inside or outside surfaces of cylinders.

II. Measurement Setup

The surface profile of the parabola is directly measured by monitoring radial deviations on the surface from the theoretical curve as a function of position along the optical axis. The equipment and experimental arrangement used to measure the optical element are shown in Figs. 2 and 3. Figure error of the element is measured mechanically using a Moore 3 measuring machine with an inductance-type electronic ball probe installed on its vertical or Z axis. The parabola is set on the slide table of the measuring machine, and a H-P 5501 interferometer monitors the movement of the slide along the X and Y axes. Figures 4 and 5 show a close-up of the parabola ready to be tested. A rotary table is attached to the slide table, and a tilt plate is mounted on the rotary table with magnets. A V-block rests on, but is not firmly attached, to, the tilt plate, and the parabola rests in the V-block with its axis parallel to the X axis and its narrow end toward the $-X$ direction. The probe is placed in contact with the inside surface of the parabola and is oriented so that it measures deviations parallel to the Y axis. Stepping motors, controlled by a set of instructions encoded on paper tape, advance the lead screws so that the parabola is stepped along the theoretical curve, which is given by

The authors are with NASA Goddard Space Flight Center, Greenbelt, Maryland 20771.

Received 14 September 1984.

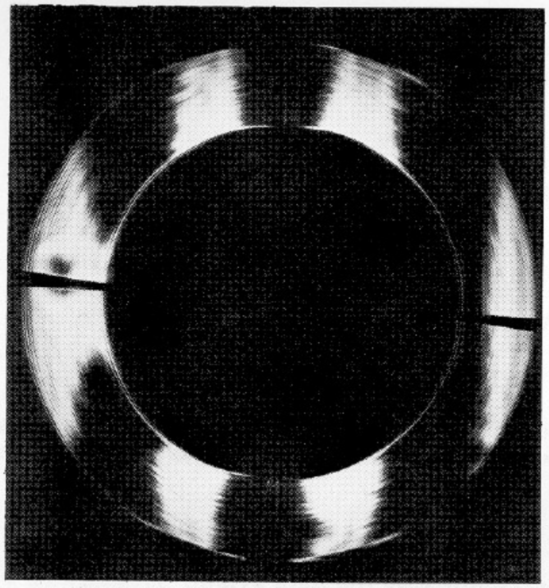

Fig. 1. Interferogram of glancing incidence mirror taken in same manner as for a normal incidence mirror. Data are compressed axially, making it difficult to interpret. The large cosine factors also make the axial positions sensitive to small errors in measuring fringe location.

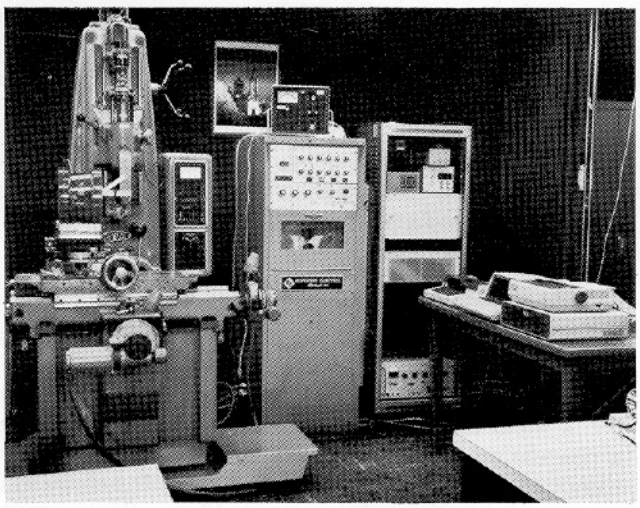

Fig. 2. Equipment used to measure glancing incidence mirrors.

$$Y = [2P(X+S) + P^2]^{1/2},$$

where Y = radial distance from optical axis to optical surface,
P = distance from the vertex of parabola to focus,
X = distance along optical axis, measured from the origin, and
S = distance from focus of parabola to the origin.

Surface deviation of the glass surface from the design curve is measured by the probe. To compensate for lead screw error and temperature expansion of the lead screw, true X and Y positions are measured with the interferometer.

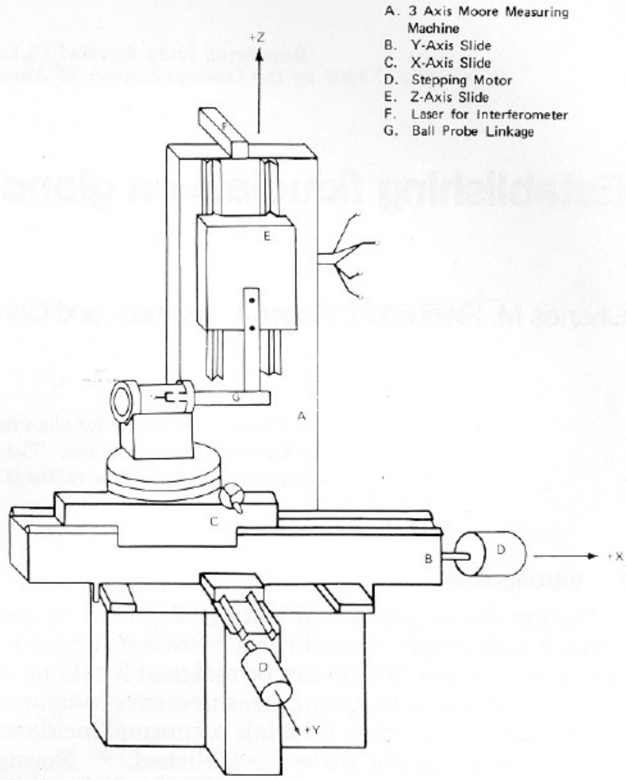

Fig. 3. Schematic diagram. Machine axes are labeled as explained in text.

The raw data consist of three measurements for each point. The interferometer measurements, X_i and Y_i, record the axial and radial positions of the mirror as it steps along the curve, and the probe measurement ΔY records the deflection of the probe at that point. The coordinates of the center of the ball on the probe are given by

$$X_p = X_i,$$
$$Y_p = Y_i - \Delta Y,$$

where X_p = axial coordinate of ball center, and Y_p = radial coordinate of ball center.

To obtain the coordinates of the glass surface, the contact point of the ball with the glass at each measurement point must be found, and the geometry for this calculation is shown in Fig. 6. The slope of the surface is first calculated by

$$dX/dY = D = [X_p(I+1) - X_p(I)]/[Y_p(I+1) - Y_p(I)],$$

where $X_p(I+1)$ = ball center axial coordinate at $(I+1)$th position,
$X_p(I)$ = ball center axial coordinate at Ith position,
$Y_p(I+1)$ = ball center radial coordinate at $(I+1)$th position, and
$Y_p(I)$ = ball center radial coordinate at Ith position.

The correction needed to obtain the axial coordinate of the glass surface from X_p is given by

$$\Delta X = r/(1+D^2)^{1/2},$$

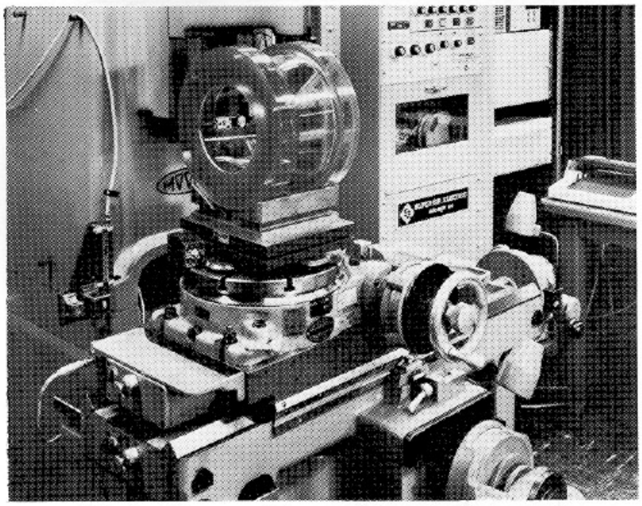

Fig. 4. Close-up of the parabola on testing mount.

A. X-Axis Slide
B. Rotary Table
C. Tilt Plate
D. V-Block
E. Parabola
F. Ball Probe

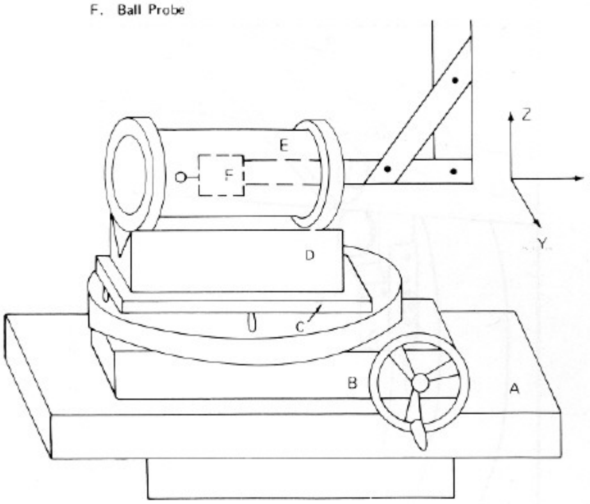

Fig. 5. Schematic diagram. Machine axes are indicated.

where ΔX = correction to X_p, and r = radius of ball center.

Finally, the glass surface coordinates are calculated by

$$X_g(I) = [X_p(I+1) + X_p(I)]/2 - \Delta X,$$

$$Y_g(I) = [Y_p(I+1) + Y_p(I)]/2 + \Delta X \cdot D,$$

where $X_g(I)$ = axial coordinate of glass surface at Ith contact point, and $Y_g(I)$ = radial coordinate of glass surface at Ith contact point. The resulting values give the axial profile of the mirror.

III. Locating Fiducials

To calculate the surface deviations from a theoretical parabola, the measurements must be referred to a coordinate system which can be reproducibly located relative to the polished surface. In this case, the reference coordinate system is cylindrical with the optical axis of the element along the axis, as shown in Fig. 7. The origin in this coordinate system is established by a pair of scratches inscribed on a ground and polished lip on the inside surface of the narrow end of the cylinder. These scratches allow precise axial and azimuthal positions to be located on the optical element. Once the coordinates of the scratch positions have been established, a third reference point, also on the ground and polished lip, can be established. The reference pad location is preselected to be a fixed distance from the axial scratch. It is chosen so that the axial slope of the radial component is zero at that point to ensure that small errors in locating the axial scratch do not introduce errors in establishing the radial reference. The radial distance of the reference pad from the optical axis has been measured so that, once it is located, the origin

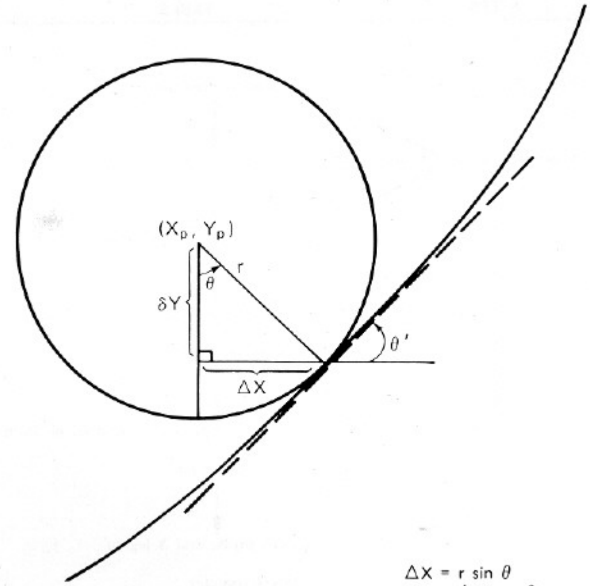

$$\Delta X = r \sin\theta$$
$$\delta Y = \Delta X/\tan\theta$$
$$\theta = \theta'$$
$$\tan\theta' = \frac{1}{dX/dY}$$

Fig. 6. Geometry of calculation of glass coordinates from position of ball center.

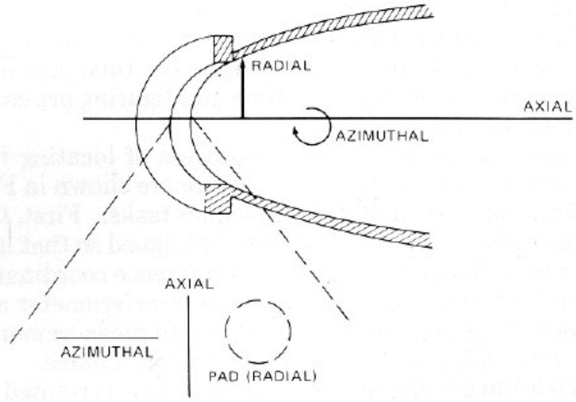

Fig. 7. Coordinate system in which figure error of mirror is expressed. Position of reference scratches on ground and polished lip is indicated. Reference pad location is also indicated.

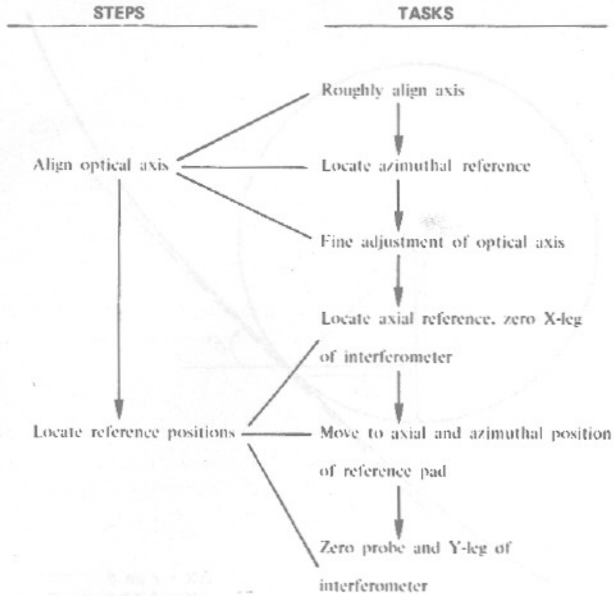

Fig. 8. Sequence of events during location of fiducials on glancing incidence mirrors. The two major tasks are shown broken down into component tasks.

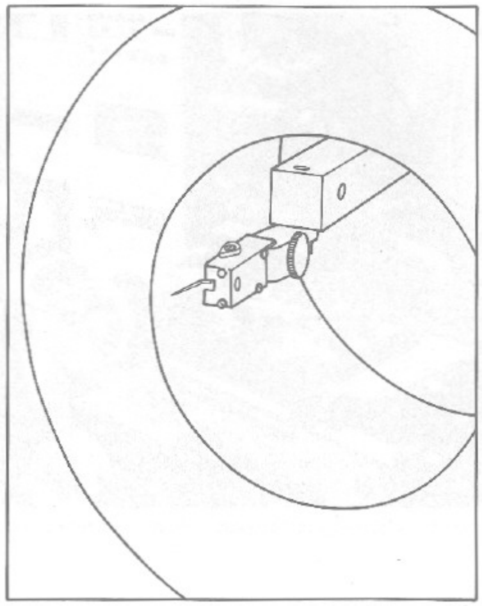

Fig. 9. Position of the electronic probe during measurement of the parabola. View is along X axis.

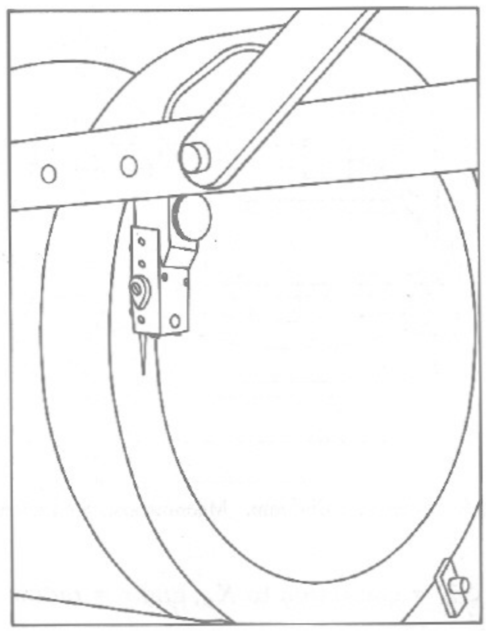

Fig. 10. Measuring tilt of the optical axis.

of the radial component in the coordinate system is established.

The reference scratches, whose positions are illustrated in Fig. 7, are inscribed after the final grinding stage. When the final polishing and figuring are completed, they are cut off.

There are two steps to the process of locating the reference scratches and pad. These are shown in Fig. 8, with each step broken into smaller tasks. First, the optical axis of the parabola must be aligned so that it is parallel with the X axis; then the reference coordinates are established, and the probe and interferometer are zeroed at these points. All subsequent measurements are made relative to these reference coordinates.

To begin the alignment, the rotary table is rotated so that the axis of the parabola is approximately parallel to the Moore X axis, and the parabola is rotated about its axis so that the pair of reference scratches is approximately at the same vertical height as the optical axis. The Y axis is then moved to bring the inside surface of the cylinder in contact with the probe, as shown in Fig. 9. Next, the probe is moved vertically until the lowest indicator reading is obtained, and the vertical position is locked at this point. This ensures that the ball contact point and probe motion are in a radial plane. Then the parabola is moved along the X axis to bring the azimuthal scratch to the axial position of the probe, after which the parabola is rotated about its axis until the probe falls into the scratch. This locates the azimuthal origin in the cylindrical coordinate system.

Once the azimuthal reference is located, fine adjustments are made to the angle of the optical axis relative to the X axis. To bring the optical axis into alignment with the X axis, the angle of the endface of the cylinder is adjusted. The angle of the endface with respect to the optical axis has been previously measured, as described in Appendix A, so that by adjusting the endface angle to the proper amount, one can bring the optical axis perpendicular to the Y and Z axes and so into alignment with the X axis.

To set the endface angle, the probe must be reoriented to measure deviations parallel to the X axis. The probe is then moved vertically until it has the same height as the optical axis and is brought into contact with the endface of the parabola on one side of the optical axis, as shown in Fig. 10. The endface has been ground flat, so that the exact radius is not important. Then the probe is zeroed, after which the parabola is

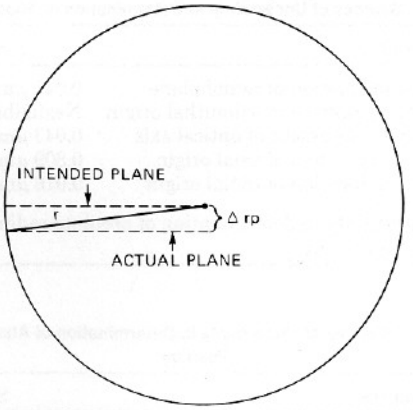

Fig. 11. If the radial plane is not located exactly, the probe will not measure along a radius of the mirror.

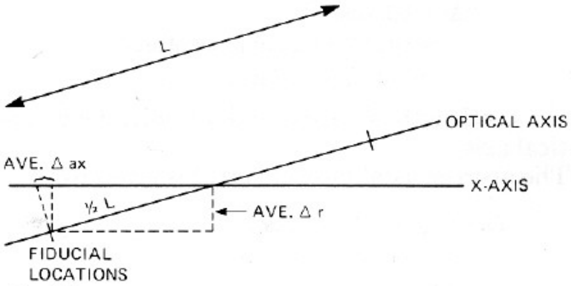

Fig. 12. Tilt of the surface caused by misalignment of the optical axis causes an average absolute radius error and an average axial position error.

moved along the Y axis until the probe contacts the endface on the other side of the optical axis. The difference between the two readings indicates the angle of the endface with respect to the Y axis. It may be adjusted by using the rotary table on which the parabola rests.

The probe is then moved vertically so that it has the same height as that portion of the endface directly above the optical axis. The parabola is moved in Y to bring the optical axis directly under the probe and then in X to zero the probe against the endface. The probe is moved in Z until it contacts that portion of the endface directly below the optical axis. The readings are compared, and the angle with respect to the Z axis is adjusted using the tilt plate. Then the angle about the Y axis is rechecked to verify that it has not changed. This has brought the optical axis perpendicular to the Y and X axes and consequently parallel to the X axis.

At this point, the azimuthal origin has been located, and the optical axis has been aligned. The next step is to establish the axial and radial origins. The probe is reoriented to measure deviations parallel to the Y axis and then is moved back into the radial plane containing the azimuthal scratch. Next, the parabola is moved in X and Y to bring the ground and polished lip into contact with the probe. Finally, the parabola is moved in X until the probe is centered in the axial reference scratch. The axial reference position has now been located, and the X-axis leg of the interferometer is zeroed at this point. To locate the reference pad, the parabola is moved 0.0254 cm (0.01 in.) in X and then moved in Y to zero the probe. The radial reference has now been located, and the Y leg of the interferometer is zeroed. The distance from the reference pad to the optical axis has been measured, as explained in Appendix B, so that any radial measurements can be referred to the optical axis by adding to them the distance from the reference pad to the optical axis.

IV. Sources of Error

Uncertainties in locating the fiducials of glancing incidence mirrors as described above lead to residual uncertainties in the absolute radius of the mirror and the absolute axial position of any feature measured on the mirror surface. The uncertainties in locating each fiducial and the effect of these uncertainties on the surface profile measurement are as follows:

A. Uncertainty in Vertical Location of the Radial Plane

The uncertainty in locating the radial plane can be determined by repeatedly locating the radial plane and noting the vertical position of the probe, as measured by the interferometer. This test shows that the radial plane may be found to within 0.00762 cm (0.003 in.). Uncertainty in the location of the radial plane will cause an uncertainty in determination of the absolute radius of the mirror. As shown in Fig. 11, the probe will not measure along a radius, and this will cause an error in radius of

$$\begin{aligned}\Delta r &= r - [r^2 - (\Delta rp)^2]^{1/2}\\ &= 7.14\ \text{cm} - [(7.14\ \text{cm})^2 - (0.00762\ \text{cm})^2]^{1/2}\\ &= 0.041\ \mu\text{m}\ (1.6\ \mu\text{in.}),\end{aligned}$$

where Δr = uncertainty in absolute radius,
r = radial location of reference pad,
Δrp = uncertainty in location of radial plane.

B. Uncertainty in Location of Azimuthal Scratch

The uncertainty in locating the azimuthal scratch is determined by repeatedly locating another scratch which was made in the same way. Interferometer readings taken after each test indicated how close the successive positions were. This set of tests shows that the bottom of the azimuthal scratch can be located to within 2.54 μm (100 μin.). This uncertainty does not introduce any error in the absolute radius, however, since the reference pad is flat in both the azimuthal and axial direction.

C. Uncertainty in Alignment of the Optical Axis

During alignment of the optical axis parallel to the X axis, the angular error can be reduced sufficiently so that there is a 0.127-μm (5-μin.) difference in probe readings across the 20.4-cm endface of the mirror. This translates into a 0.13-sec of arc error in the alignment of the optical axis, causing a tilt in the measured surface. This tilt will contribute an average absolute radius error and average error in absolute axial position, as shown in Fig. 12. The average absolute radius error is given by

$$\Delta r = \tfrac{1}{2} L \sin\alpha$$
$$= \tfrac{1}{2}(13.7\ \text{cm}) \sin(0.13\ \text{sec of arc})$$
$$= 0.043\ \mu\text{m} = 1.7\ \mu\text{in.},$$

where L = length of mirror, and α = alignment error of optical axis.

The average axial position error is given by

$$\Delta ax = \tfrac{1}{2} \cdot L - \tfrac{1}{2} \cdot L \cos\alpha$$
$$= \tfrac{1}{2}(13.7\ \text{cm})[1 - \cos(0.13\ \text{sec of arc})]$$
$$\cong 0.$$

D. Uncertainty in Location of the Axial Scratch

The uncertainty in locating the axial scratch is determined in the same manner as the uncertainty in finding the azimuthal scratch and is found to be 2.54 μm (100 μin.). This error contributes an error to both the absolute radius measurement and the absolute axial position. The error in axial position is just the uncertainty in finding the scratch, or 2.54 μm. The uncertainty in the absolute radius can be calculated by averaging the errors in radial position at each end caused by the uncertainty in axial position. The radial error at a given axial position is

$$\Delta r = \Delta ax[2p/(2p(x+s)+p^2)^{1/2}],$$

where p = vertex radius of curve = 1.07398 cm,
x = axial position, and
s = distance of axial scratch from focus = 13.82 cm.

The average radial uncertainty at two axial positions, x and x_2, is

$$\overline{\Delta r} = \tfrac{1}{2}\{\Delta ax \cdot 2p/[2p(x_1+s)+p^2]^{1/2} + \Delta ax \cdot 2p/[2p(x_2+s)+p^2]^{1/2}\}.$$

Substituting in the values $x_1 = 0.91$ cm and $x_2 = 16.9$ cm gives the average error in absolute radius:

$$\Delta r = 0.81\ \mu\text{m}\ (31.9\ \mu\text{in.}).$$

E. Uncertainty in Location of Reference Pad

The precision in locating the reference pad is limited by the precision in the measuring instrument, which is 0.016 μm (0.6 μin.). This contributes an uncertainty of 0.016 μm to the determination of absolute radius.

These errors are summarized in Tables I and II. The overall uncertainty in the absolute radius of the mirror is 0.812 μm (32.0 μin.), and the overall uncertainty in absolute axial position is 2.54 μm (100 μin.).

V. Summary

The procedure described allows a reference coordinate system to be defined by using reference marks inscribed on the glass, in which figure error measurements of cylindrical glancing incidence mirrors can be made. These fiducials allow the surface deviations to be mapped reproducibly onto the surface of the optical element.

Appendix A

To obtain the angle of the endface relative to the optical axis, the optical axis must first be aligned to one of the machine axes; here the Z axis. Then the measurement of the angle of the endface relative to the Z axis will also indicate the angle of the endface relative to the optical axis. The sequence of operations for this measurement is shown in Fig. 13.

Table I. Sources of Uncertainty in Determination of Absolute Radius

Source	Size
Uncertainty of location of radial plane	0.041 μm (1.6 μin.)
Uncertainty in location of azimuthal origin	Negligible
Uncertainty in alignment of optical axis	0.043 μm (1.7 μin.)
Uncertainty in location of axial origin	0.809 μm (31.9 μin.)
Uncertainty in location of radial origin	0.016 μm (0.6 μin.)

Overall uncertainty in determination of absolute radius = 0.812 μm (32.0 μin.)

Table II. Sources of Uncertainty in Determination of Absolute Axial Position

Source	Size
Uncertainty in alignment of optical axis	Negligible
Uncertainty in location of axial origin	2.54 μm (100 μin.)

Overall uncertainty in determination of absolute axial position = 2.54 μm (100 μin.)

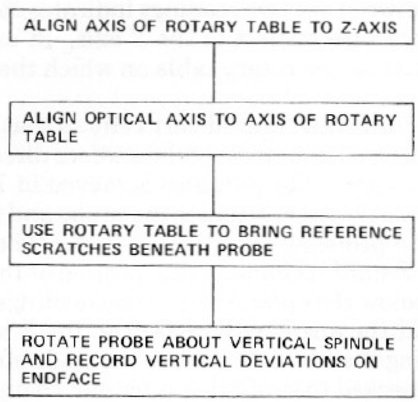

Fig. 13. Sequence of events during measurement of angle of endface relative to the optical axis.

In preparation for alignment of the optical axis to the Z axis, a rotary table is aligned to this axis. The rotary table is attached to the slide table so that its axis is approximately coincident with the Z axis. A precision convex sphere is placed on the rotary table, and the probe is lowered and extended so that it contacts the outside surface of the sphere. The sphere is positioned on the rotary table until the probe shows no deviations as the sphere is rotated using the rotary table. This places the vertex of the sphere on the axis of the rotary table. Next the rotary table is moved along the X and Y axes so that the probe shows no deviations as it is rotated about the Z axis. This places the vertex of the sphere on the Z axis and in turn the axis of the rotary table in coincidence with the Z axis.

Next, the parabola is aligned so that its axis is parallel to and coincident with the Z axis. A tilt plate is attached to the rotary table using magnets, and the parabola is set, narrow end down, on the tilt plate. The probe is lowered and extended so that it contacts the inside surface of the parabola. The probe is oriented to measure deviations transverse to the Z axis, in other words, deviations radial to the optical axis. A motor on the spindle drives the probe azimuthally around the inside surface of the parabola, and a circular chart recorder records the radial deviations measured by the probe. Two such tracings are made, one at an axial position near the wide end of the parabola, and one at an axial position near the narrow end of the parabola. If the optical axis is not parallel to the Z axis, the two traces will not be mutually concentric. This can be remedied by adjusting the angle of the tilt plate. When the optical axis has been aligned parallel to the Z axis, it can be checked for coincidence with the Z axis by taking two tracings as above and checking whether they are concentric with the center of the chart paper. This may be adjusted by sliding the parabola across the top of the tilt plate. Once the tracings at either end of the parabola are concentric with each other and with the center of the chart paper, the optical axis is parallel to and coincident with the Z axis.

Once the optical axis has been aligned to the Z axis, the magnitude and orientation of the angle of the endface relative to the Z axis can be measured. The probe is moved up out of the parabola and is reoriented to measure displacements parallel to the Z axis. It is extended and lowered so that it contacts the annular end of the cylindrical blank. The rotary table is rotated to bring the pair of reference scratches on the lip inside the cylinder to the azimuthal position of the probe, and the starting position of the pen is marked on the chart paper. The spindle motor and the chart recorder are simultaneously started, and the vertical deviations of the endface are recorded as the probe is driven azimuthally around the endface. The angle of the endface relative to the Z axis, and hence to the optical axis, is indicated by the deviations of the probe as read from the circular chart.

The probe deviations indicating the angle of the endface relative to the optical axis are broken down into two convenient components. One component lies in the plane defined by the reference scratches and the optical axis. The deviation along this plane can be determined by drawing a line on the chart paper through the center of the chart and the mark denoting the reference scratches and taking the difference of the deviations from zero along this line. The second component is obtained by taking the difference of the deviations along an orthogonal line on the chart paper. The endface angle measurements are now in a convenient form for aligning the optical axis prior to figure error measurements.

Appendix B

There is no physical object on the optical axis of the parabola; thus the measurement of the distance from the reference pad to the optical axis must be done indirectly. The optical axis must first be aligned parallel to and coincident with the Z axis. Then the distance

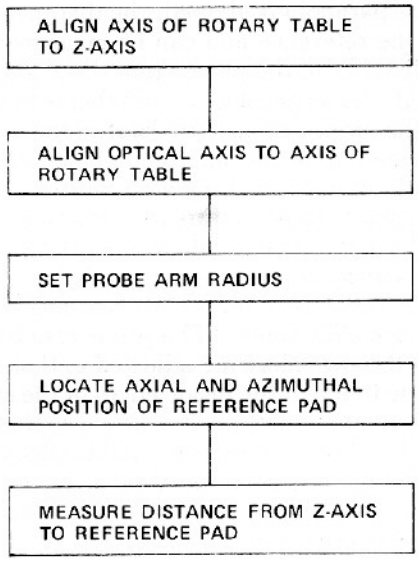

Fig. 14. Sequence of events during measurement of distance from optical axis to reference pad.

from the reference pad to the Z axis can be measured, and this in turn will give the distance of the reference pad from the optical axis. The sequence of events is shown in Fig. 14.

The first step in the procedure is to align the axis of the parabola. A rotary table is attached to the slide table of the Moore machine, and its axis is aligned coincident with the Z axis, as explained in Appendix A. The coordinates of the slide table are read from the indicators on the X- and Y-axis lead screws and are recorded, and the X leg of the interferometer is zeroed at this point. A tilt plate is attached to the rotary table, and the parabola is set, narrow end down, on the tilt plate. The probe is oriented to measure displacements parallel to the Z axis and is brought into contact with the annular end of the cylindrical blank. The probe is rotated about the Z axis until it has the same azimuthal position as the reference scratches, and the probe is zeroed at this point. Then the probe is rotated about the Z axis through 180°, and the deviation from zero at this new position is measured. The angle between the endface of the cylinder and the optical axis has been measured, and the tilt plate is adjusted so that the reading equals the deviation necessary to correct for that component of the endface angle. Then the probe is rotated about the Z axis through 90°, is zeroed, and the above procedure is repeated to correct for the component of the endface angle orthogonal to the first. This aligns the optical axis parallel to the Z axis. The optical axis must now be moved into coincidence with the Z axis. The probe is reoriented to measure deviations perpendicular to the optical axis. Its arm length and height are adjusted to bring it into contact with the inside surface of the parabola. Then the probe is rotated about the Z axis, and the parabola is positioned on the tilt plate until the probe shows no deviations as it sweeps azimuthally around the parabolic surface. This places the optical axis into coincidence with the Z axis of the machine.

Once the parabola is aligned, the distance from the Z axis to the reference pad can be measured. To do this, the distance of the probe from the Z axis must be determined. The easiest way to do that is to adjust the radius of the probe arm to a predetermined distance, in this case, one-half of the length of a 15-cm (6-in.) gage block, with correction for temperature expansion. Figure 15 shows the procedure for adjusting the radius of the probe arm. The parabola is moved along the X and Y axes away from the probe and the 15-cm gage block, with small gage blocks wrung onto its ends, is placed on the slide table. The probe arm length and position of the gage block are adjusted so that the probe can be made to touch the inside edges of the small gage blocks as it rotates about the Z axis and so that it zeroes at both ends. At this point, the outside edge of the ball will be a distance Y_a from the Z axis, where Y_a equals one-half of the length of the 15-cm gage block.

Once the length of the probe arm has been adjusted, the probe must be oriented so that it measures deviations parallel to the X axis so that adjustments in the position of the slide table needed to zero the probe will only be made along one machine axis. This is done by first adjusting a gage block parallel to the Y axis and thus perpendicular to the X axis.

This operation is begun by placing a 7.5-cm (3-in.) gage block on the slide table, approximately parallel to the Y axis. The probe is brought into contact with the vertical side of the gage block, as shown in Fig. 16. The gage block is adjusted until the probe shows no deviation as the gage block is moved in Y, thus aligning it parallel to the Y axis. The probe is then rotated about the Z axis against the gage block, as shown in Fig. 17, until the highest indicator reading is obtained, at which point the spindle is locked. The probe has now been adjusted to measure deviations parallel to the X axis.

Finally, the parabola is moved back to the position at which the optical axis is aligned with the Z axis. The probe is lowered so that it contacts the parabolic surface. The probe is moved vertically to the height of the reference scratch that determines the azimuthal position, which will be vertical with the parabola on its end. If the parabola must be moved to keep the probe readings on scale, it must be moved only along the X axis so that the direction from the probe to the optical axis is parallel to the direction in which the probe measures deviations. The rotary table is then rotated until the probe is centered in the scratch, establishing the azimuthal position. Then the probe is moved vertically until it is centered in the scratch denoting axial position, which will be horizontal with the parabola on its end. This locates the reference axial position on the parabola and allows the reference pad to be located.

The reference pad has the same azimuthal position as the reference scratches, so that it is only necessary to move axially to locate it. After the probe has been moved vertically to the proper axial position, it is zeroed by moving the parabola along the X axis. Because the distance from the reference pad to the optical axis does not equal the length of the probe arm, the optical axis will no longer be coincident with the Z axis. The displacement between the Z axis and the optical axis, as read from the X leg of the interferometer, indicates the amount of correction needed to obtain the reference pad radial location from the probe arm length, that is,

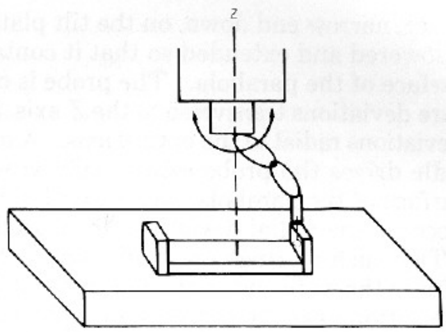

Fig. 15. Adjusting length of probe arm. The probe rotates about the Z axis.

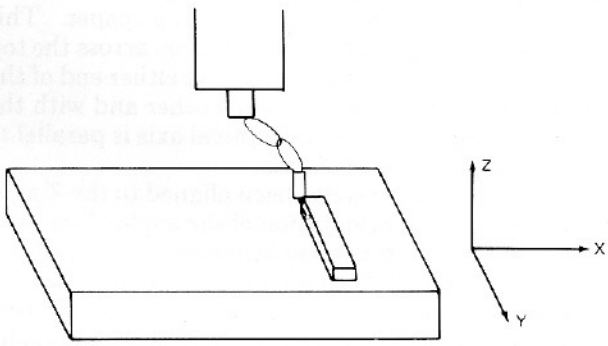

Fig. 16. Aligning gage block parallel to Y axis. Machine axes are indicated.

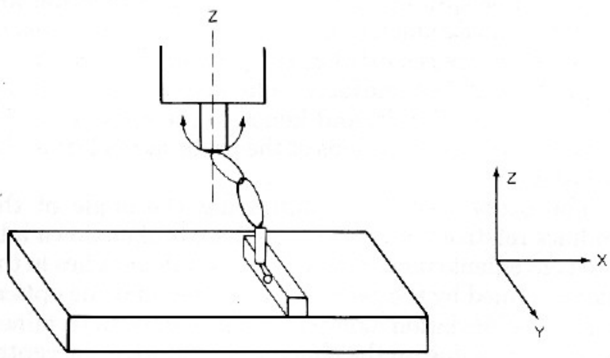

Fig. 17. Orienting probe to measure displacements parallel to X axis. Machine axes are indicated. Probe rotates about Z axis.

$$Y_r = Y_a - \Delta X,$$

where Y_r = distance from optical axis to reference pad,

Y_a = length of probe arm, and

ΔX = reading from X leg of interferometer.

References

1. A. F. Slomba, "Development of an Accurate Mirror Fiducial System Compatible with Computer Controlled Polishing," Proc. Soc. Photo-Opt. Instrum. Eng. **192,** 121 (19xx).
2. M. P. Rimmer, C. M. King, and D. G. Fox, "Computer Program for the Analysis of Interferometric Data," Appl. Opt. **11,** 2790 (1972).
3. M. Ruda, "Alignment of Off-Axis Aspheric Surfaces," Proc. Soc. Photo-Opt. Instrum. Eng. **251,** 29 (19xx).
4. C. M. Fleetwood and J. D. Mangus, "Fabrication of an Extreme Ultraviolet Glancing Incidence Telescope," Opt. Eng. 159 (Mar./Apr. 1974).
5. W. M. Neupert *et al.*, "A Solar Extreme Ultraviolet Telescope and Spectrograph for Shuttle/Spacelab," Space Sci. Rev. **2a,** 425 (1981).
6. W. M. Neupert, "A Solar Extreme Ultraviolet Telescope and Spectrograph for Space Shuttle," NASA Tech. Memor. 80643 (Nov. 1978).